

文章编号: 1006-9941(2012)05-0505-09

The Thermal Safety and a Density Functional Theoretical Study on *N,N'*-Bis[*N*-(2,2,2-Trinitroethyl)-*N*-Nitro]Ethylenediamine (BTNEDA)

HU Rong-zu^{1,3}, ZHAO Feng-qi¹, GAO Hong-xu¹, MA Hai-xia², ZHANG Hai³, XU Kang-zhen², ZHAO Hong-an⁴, YAO Er-gang¹

(1. Science and Technology on Combustion and Explosion Laboratory, Xi'an Modern Chemistry Research Institute, Xi'an 710065, China; 2. College of Chemical Engineering, Northwest University, Xi'an 710069, China; 3. Department of Mathematics/Institute of Data Analysis and Computation Chemistry, Northwest University, Xi'an 710069, China; 4. College of Communication Science and Engineering, Northwest University, Xi'an 710069, China)

Abstract: With the help of the constant-volume standard combustion heat (Q_c) of *N,N'*-bis[*N*-(2,2,2-trinitroethyl)-*N*-nitro]ethylenediamine (BTNEDA), the initial temperature (T_0), at which DSC curves deviates from the baseline, the onset temperature (T_e) and maximum peak temperature (T_p) from the non-isothermal DSC curves at different heating rates (β), the thermal decomposition activation energy (E_k and E_O) and pre-exponential constant (A_K) obtained by Kissinger's method and Ozawa's method, the value of $b_{e0(or p0)}$ from equation $\ln\beta_i = \ln[A_0/b_{e0(or p0)}G(\alpha)] + b_{e0(or p0)}T_{e(or p)i}$ and the value of $a_{e0(or p0)}$ from equation $\ln\beta_i = \ln[A_0/(a_{e0(or p0)} + 1)G(\alpha)] + (a_{e0(or p0)} + 1)\ln T_{e(or p)i}$, the value of b from equation $\ln\left(\frac{\beta_i}{T_{ei} - T_{0i}}\right) = \ln\left(\frac{A_0}{G(\alpha)}\right) + bT_{ei}$, the value of a from equation $\ln\left(\frac{\beta_i}{T_{ei} - T_{0i}}\right) = \ln\left(\frac{A_0}{G(\alpha)}\right) + a\ln T_{ei}$, the estimated values of specific heat capacity (c_p), density (ρ) and thermal conductivity (λ), the decomposition heat (Q_d , taking half-explosion heat), Zhang-Hu-Xie-Li formula, Hu-Yang-Liang-Xie formula, formulae of calculating the critical temperature of thermal explosion based on Berthelot's equation and Harcourt-Esson's equation, Smith's equation, Friedman's formula, Bruckman-Guillet formula, thermodynamic formulae and Wang-Du formulas, the constant-volume standard combustion energy $\Delta_c U_{(BTNEDA,s,298.15K)}$ and standard enthalpy of formation $\Delta_f H_m^\theta_{(BTNEDA,s,298.15K)}$ obtained by ideal combustion reaction and Hess's law, the values (T_{00} , T_{e0} and T_{p0}) of T_0 , T_e and T_p corresponding to $\beta \rightarrow 0$, critical temperature of thermal explosion (T_{be0} and T_{bp0}), adiabatic time-to-explosion (t_{lad}), 50% drop height (H_{50}) of impact sensitivity, critical temperature of hot-spot initiation (T_{cr}), thermal sensitivity probability density function $S(T)$ for infinite platelike, infinite cylindrical and spheroidal BTNEDA with half thickness and radius of 1 m surrounded with surrounding of 350 K, peak temperature corresponding to the maximum value of $S(T)$ vs T relation curve ($T_{S(T)max}$), safety degree (SD), critical thermal explosion ambient temperature (T_{acr}) and thermal explosion probability (P_{TE}) of BTNEDA were calculated. The following results of evaluating the thermal safety of BTNEDA were obtained: (1) $\Delta_c U_{(BTNEDA,s,298.15K)} = -(3478.11 \pm 6.41) \text{ kJ} \cdot \text{mol}^{-1}$ and $\Delta_f H_m^\theta_{(BTNEDA,s,298.15K)} = -(53.54 \pm 6.41) \text{ kJ} \cdot \text{mol}^{-1}$; (2) $T_{00} = 438.73 \text{ K}$, $T_{SADT} = T_{e0} = 440.73 \text{ K}$, $T_{p0} = 446.53 \text{ K}$; $T_{be0} = 449.88 \text{ K}$, $T_{bp0} = 455.28 \text{ K}$; (3) when $E_k = 199.5 \text{ kJ} \cdot \text{mol}^{-1}$, $A_K = 10^{20.45} \text{ s}^{-1}$, $c_p = 1.12 \text{ J} \cdot \text{g}^{-1} \cdot \text{K}^{-1}$, $Q_d = 3226 \text{ J} \cdot \text{g}^{-1}$, $T_0 = T_{e0} = 440.73 \text{ K}$, $T = T_b = 455.26 \text{ K}$, $f(\alpha) = 3(1 - \alpha)^{2/3}$, $a = 10^{-3} \text{ cm}$, $\rho = 1.87 \text{ g} \cdot \text{cm}^{-3}$, $t - t_0 = 10^{-4} \text{ s}$, $T_{room} = 293.15 \text{ K}$ and $\lambda = 0.00269 \text{ J} \cdot \text{cm}^{-1} \cdot \text{s}^{-1} \cdot \text{K}^{-1}$, $H_{50} = 15.03 \text{ cm}$, $t_{lad} = 1.25 \text{ s}$, $T_{cr,hot,spot} = 333.86 \text{ K}$, for infinite plate, $T_{S(T)max} = 350 \text{ K}$, $T_{acr} = 345.47 \text{ K}$, $SD = 28.55\%$, $P_{TE} = 71.45\%$, for infinite cylinder, $T_{S(T)max} = 354.5 \text{ K}$, $T_{acr} = 349.73 \text{ K}$, $SD = 39.31\%$, $P_{TE} = 60.69\%$, for sphere, $T_{S(T)max} = 357.00 \text{ K}$, $T_{acr} = 352.42 \text{ K}$, $SD = 45.81\%$, $P_{TE} = 54.19\%$. The conjunction of BTNEDA was optimized with density functional theory (DFT) B3LYP. The atomic charges, total energy and frontier orbital energy were also discussed.

Key words: physical chemistry; *N,N'*-bis[*N*-(2,2,2-trinitroethyl)-*N*-nitro]ethylenediamine (BTNEDA); thermal decomposition; thermal safety; self-accelerating decomposition temperature; critical temperature of thermal explosion; adiabatic time-to-explosion; impact sensitivity; critical temperature of hot-spot initiation; safety degree; critical thermal explosion ambient temperature; thermal explosion probability; the quantum chemical calculation

CLC number: TJ55,O643

Document code: A

DOI: 10.3969/j.issn.1006-9941.2012.05.001

1 Introduction

N,N'-Bis[*N*-(2,2,2-trinitroethyl)-*N*-nitro]ethylenediamine (BTNEDA) is a typical nitramine compound. Its crystal density is $1.87 \text{ g} \cdot \text{cm}^{-3}$. The detonation velocity is about $8970 \text{ m} \cdot \text{s}^{-1}$ ($\rho = 1.842 \text{ g} \cdot \text{cm}^{-3}$). Therefore, BTNEDA is used as high explosive. Its explosion and combustion properties^[1] and thermal and kinetic behavior under isothermal and non-isothermal conditions have been reported^[2-6]. In the present work, we report its thermal safety and the theoretical results obtained by the quantum chemical investigation method.

This is quite useful in the evaluation of its heat-resistance ability under non-isothermal condition and in the exploration of its phenomenon, mechanism and process from thermal decomposition to thermal explosion. The theoretical calculation was also performed for further studying the relationship between the structure and properties of this material.

2 Experimental

2.1 Material

BTNEDA was prepared in Xi'an Modern Chemistry Research Institute. The compound was purified by recrystallization from nitromethane. Its structure was characterized by elemental analyses, IR spectrometry, mass spectrometry and nuclear magnetic resonance spectrometry. Its purity was more than 99.5%. The sample was kept in a vacuum desiccator before use.

Received Date: 2012-05-21; Revised Date: 2012-06-24

Project Supported: National Natural Science Foundation of China (No. 21073141; No. 21173163)

Biography: HU Rong-zu (1938 -), male, professor, research-fields: thermochemistry and thermoanalysis. e-mail: hurongzu88@163.com

2.2 Apparatus and Experimental Conditions

DSC apparatus, highly-sensitive Bourdon glass membrane manometer and their operating procedure and conditions used in experiment and the principal and method of collecting, analyzing and treating the data from DSC curves and pressure(p)-time(t) curves were the same as those in Refs [3,4,7-9].

2.3 The quantum chemical investigation

Many studies^[10-12] have shown that the density functional theory (DFT) methods, especially the B3LYP hybrid model, in combination with the basis set 6-311 + + G**^[13-15] can produce reliable geometries, energies and infrared vibrational frequencies. The initial geometry of BTNEDA generated from Chem3D software was fully optimized at the DFT-B3LYP level by the Bery method with 6-311 + + G** basis set. The scaled IR frequencies were calibrated by multiplying 0.96^[16]. All calculations were carried out on an IBM P4 computer with Gaussian-03W^[17] program.

3 Results and discussion

3.1 Specific heat capacity c_p and thermal conductivity λ

Assuming that $c_p = 0.8c_v$ and substituting the values of M of 476.19 and a , b , c and d in Eq. (1) into Eq. (2),

$$C_aH_bO_cN_d = C_6H_8O_{16}N_{10} \quad (1)$$

$$c_v = \left\{ \frac{3R(a+b+c+d)}{2M} \times \left[1 + \frac{2c^2}{(4a+b)(a+b+c+d)} - \frac{2ac^2}{(4a+b)(a+b+c+d)^2} \right] \right\} \quad (2)$$

we obtain $c_p = 0.8c_v = 1.12 \text{ J} \cdot \text{g}^{-1} \cdot \text{K}^{-1}$

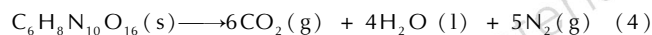
By substituting the values of c_p of $1.12 \text{ J} \cdot \text{g}^{-1} \cdot \text{K}^{-1}$, ρ of $1.87 \text{ g} \cdot \text{cm}^{-3}$, T_m of 453.15 K and M of 476.19 into Eq. (3)^[18].

$$\lambda = \frac{3.7287 \times 10^{-5} c_p^{3.0116} \rho^{0.9279}}{T_m^{-0.7652} M^{0.2158}} \quad (3)$$

the value of λ of $0.269 \text{ W} \cdot (\text{m} \cdot \text{K})^{-1}$ was obtained.

3.2 STANDARD COMBUSTION ENERGY

The standard combustion enthalpy of BTNEDA, $\Delta_c H_m^\theta$ (BTNEDA,s,298.15K), was referred to the combustion enthalpy change of the following ideal combustion reaction at 298.15 K and 100 kPa.



The standard combustion energy of BTNEDA, $\Delta_c U$ was calculated by the following equations:

$$\Delta_c H_m^\theta \text{ (BTNEDA,s,298.15K)} = \Delta_c U \text{ (BTNEDA,s,298.15K)} + \Delta n RT \quad (5)$$

$$\Delta n = n_g \text{ (products)} - n_g \text{ (reactants)} \quad (6)$$

where $\Delta_c H_m^\theta = -(Q_c) = -(3450.84 \pm 6.41)^{[1]}$, n_g is the total amount in mole of gases present as products or as reactants, $\Delta n = 6 + 5 = 11$, $R = 8.314 \text{ J} \cdot \text{K}^{-1} \cdot \text{mol}^{-1}$, $T = 298.15 \text{ K}$. The result is $-(3478.11 \pm 6.41) \text{ kJ} \cdot \text{mol}^{-1}$.

3.3 STANDARD ENTHALPY OF FORMATION

The standard enthalpy of formation of BTNEDA, $\Delta_f H_m^\theta$ (BTNEDA,s,298.15K), was calculated by Hess's law according to the thermochemical equation (7):

$$\Delta_f H_m^\theta \text{ (BTNEDA,s,298.15K)} = 6\Delta_f H_m^\theta \text{ (CO}_2\text{,g,298.15K)} + 4\Delta_f H_m^\theta \text{ (H}_2\text{O,l,298.15K)} - \Delta_c H_m^\theta \text{ (BTNEDA,s,298.15K)} \quad (7)$$

when $\Delta_f H_m^\theta \text{ (CO}_2\text{,g,298.15K)} = (-393.51 \pm 0.13) \text{ kJ} \cdot \text{mol}^{-1}$, $\Delta_f H_m^\theta \text{ (H}_2\text{O,l,298.15K)} = (-285.83 \pm 0.042) \text{ kJ} \cdot \text{mol}^{-1}$, the results obtained is $-(53.54 \pm 6.41) \text{ kJ} \cdot \text{mol}^{-1}$.

3.4 Explosion properties

By substituting the values of a , b , c and d in $C_aH_bO_cN_d = C_6H_8N_{10}O_{16}$, $\beta = 1.87 \text{ g} \cdot \text{cm}^{-3}$, $\Delta_f H_m^\theta = -53.54 \text{ kJ} \cdot \text{mol}^{-1}$ into Kamlet-Jacobs equations (8) ~ (12):

$$D = 1.01 (NM^{1/2} Q^{1/2})^{1/2} (1 + 1.30\rho) \quad (8)$$

$$p = 1.558 NM^{1/2} Q^{1/2} \rho^2 \quad (9)$$

$$N = \frac{b+2d+2c}{4M} \quad (10)$$

$$M = \frac{4M}{b+2c+2d} \quad (11)$$

$$Q = 4.184 \times \left(\frac{28.9b + 94.05a + 0.239\Delta_f H_m^\theta}{M} \right) \times 10^{-3} \quad (12)$$

where D is detonation velocity, $\text{km} \cdot \text{s}^{-1}$; p is detonation pressure, GPa; N is moles of gases detonation products per gram of explosive; M is average molecular weight of gaseous products; Q is chemical energy of detonation, $\text{J} \cdot \text{g}^{-1}$; ρ is density of explosives, $\text{g} \cdot \text{cm}^{-3}$; and $\Delta_f H_m^\theta$ is standard enthalpy of formation, the values of D of $9.298 \text{ km} \cdot \text{s}^{-1}$, p of 39.23 GPa , N of $0.0315 \text{ mol} \cdot \text{g}^{-1}$, M_g of $31.73 \text{ g} \cdot \text{mol}^{-1}$, Q of $6879.7 \text{ J} \cdot \text{g}^{-1}$ are obtained.

3.5 Thermal behavior

A typical DSC curve for BTNEDA is shown in Fig. 1. DSC curve consists of one endothermic peak and one exothermic peak. The endothermic peak at 180°C is the phase change from solid to liquid, while the exothermic peak at 197°C is caused by the decomposition reaction.

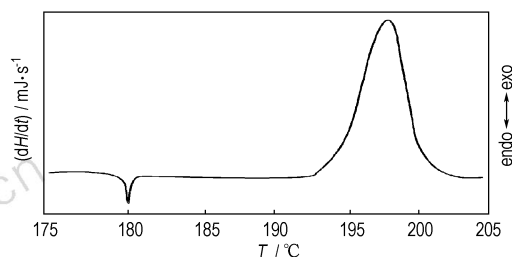


Fig. 1 DSC curve for BTNEDA at a heating rate of $10^\circ \text{C} \cdot \text{min}^{-1}$

3.6 Kinetic parameters based on initial temperature, onset temperatures and peak temperatures at different heating rates

In order to obtain the kinetic parameters (the apparent activation energy E_a and pre-exponential constant A) of the exothermic decomposition reaction of BTNEDA, a multiple heating (method Kissinger's method^[19]) [Eq. (13)] is employed. From the original data in Table 1, the value of E_K is determined to be $199.50 \text{ kJ} \cdot \text{mol}^{-1}$. The value of A_K is $10^{20.45} \text{ s}^{-1}$. The linear correlation coefficient r_K is 0.9976. The values of E_{op} and E_{oe} obtained by Ozawa's method^[20] [Eq. (14)] are 197.03 and $183.98 \text{ kJ} \cdot \text{mol}^{-1}$, respectively. The values of r_{op} and r_{oe} are 0.9978 and 0.9967, respectively.

The values of b_{e0} , b_{p0} , a_{e0} and a_{p0} obtained by Eqs. (15) and (16) and the values of b , a and E obtained by Eqs. (17), (18) and (19) are shown in Table 1.

Table 1 The original data of BTNEDA determined by non-isothermal DSC and kinetic parameters of thermal decomposition reaction obtained by Kissinger's method, Ozawa's method and Eqs. (15), (16), (17), (18) and (19)

initial data				calculated values ²⁾																
β K·min ⁻¹ /K	T_0 /K	T_e /K	T_p ¹⁾ /K	T_{00} /K	T_{e0} /K	T_{p0} /K	Kissinger's method			Ozawa's method				Eq. (15)		Eq. (16)		Eq. (17)	Eq. (18)	Eq. (19)
							E_K /kJ·mol ⁻¹	$\lg(A_K/s^{-1})$	r_K	E_{op} /kJ·mol ⁻¹	r_{op}	E_{oe} /kJ·mol ⁻¹	r_{oe}	$b_{e0}^{(3)}$ r_{e0}	$b_{p0}^{(3)}$ r_{p0}	$a_{e0}^{(4)}$ r_{e0}	$a_{p0}^{(4)}$ r_{p0}	$b^{(5)}$ r_b	$a^{(6)}$ r_a	$E^{(7)}$ /kJ·mol ⁻¹
1.053	443.15	445.15	450.15	438.73	440.73	446.53	199.50	20.45	0.9976	197.03	0.9978	183.98	0.9967	0.1108	0.1162	49.78	52.83	0.1108	50.78	193.46
2.105	451.15	453.15	457.15											0.9976	0.9977	0.9972	0.9978	0.9976	0.9972	0.9976
5.294	458.15	460.15	463.15																	
10.56	465.15	467.15	470.15																	
20.63	470.15	472.15	476.15																	

Note: 1) cited from Reference [3].

2) E , apparent activation energy; A , pre-exponential constant; Subscript K, data obtained by Kissinger's method^[19]; Subscript O: data obtained by Ozawa's method^[20].3) The value of $b_{e0(or p0)}$ is from $\ln\beta_i$ vs. $T_{e(or p)i}$ relation in Eq. (15).4) The value of $a_{e0(or p0)}$ is from $\ln\beta_i$ vs. $\ln T_{e(or p)i}$ relation in Eq. (16).5) The value of b is from $\ln\left(\frac{\beta_i}{T_{ei} - T_{0i}}\right)$ vs. T_{ei} relation in Eq. (17).6) The value of a is from $\ln\left(\frac{\beta_i}{T_{ei} - T_{0i}}\right)$ vs. $\ln T_{ei}$ relation in Eq. (18).7) The value of E is from $\ln\left(\frac{\beta_i}{T_{ei} - T_{0i}}\right)$ vs. $1/T_{ei}$ relation in Eq. (19).

$$\ln\left(\frac{\beta_i}{T_{pi}^2}\right) = \ln\left[\frac{A_K R}{E_K} - \frac{E_K}{R T_{pi}}\right] \quad (13)$$

$$\lg\beta_i = \lg\left[\frac{A_K E_{oe(or op)}}{RG(\alpha)}\right] - 2.315 - 0.4567 \frac{E_{oe(or op)}}{RT_{o(or p)i}} \quad (14)$$

$$\ln\beta_i = \ln\left[\frac{A_0}{b_{e0(or p0)} G(\alpha)}\right] + b_{e0(or p0)} T_{e(or p)i} \quad (15)$$

$$\ln\beta_i = \ln\left[\frac{A_0}{(a_{e0(or p0)} + 1) G(\alpha)}\right] + (a_{e0(or p0)} + 1) \ln T_{e(or p)i} \quad (16)$$

$$\ln\left(\frac{\beta_i}{T_{ei} - T_{0i}}\right) = \ln\left[\frac{A_0}{G(\alpha)}\right] + b T_{ei} \quad (17)$$

$$\ln\left(\frac{\beta_i}{T_{ei} - T_{0i}}\right) = \ln\left[\frac{A_0}{G(\alpha)}\right] + a \ln T_{ei} \quad (18)$$

$$\ln\left(\frac{\beta_i}{T_{ei} - T_{0i}}\right) = \ln\left[\frac{A_0}{G(\alpha)}\right] - \frac{E}{RT_{ei}} \quad (19)$$

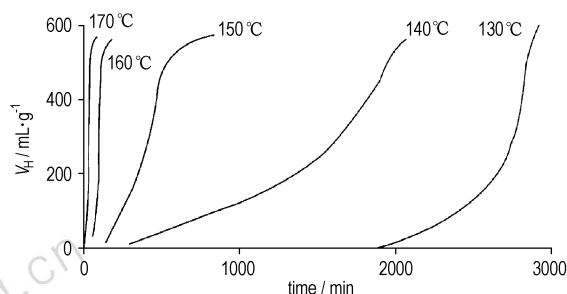
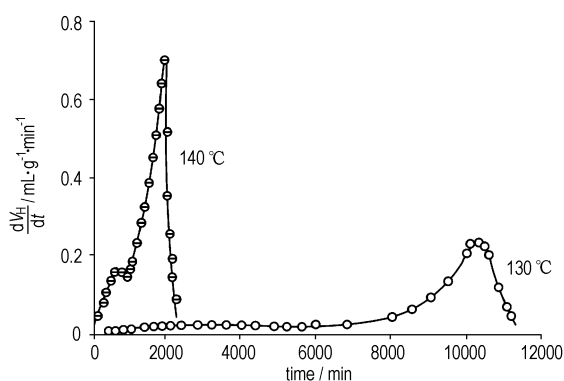
3.7 Apparent activation energy of decomposition reaction at 130–170 °C

To verify the reliability of the values of E_K , E_{op} and E_{oe} , we measured the thermal decomposition processes of BTNEDA under the conditions of vacuum and low loading density at 130 °C, 140 °C, 150 °C, 160 °C and 170 °C, using a highly sensitive Bourdon glass membrane manometer and calculated the characteristic data, induction period (t_{in}), half decomposition period ($t_{1/2}$), initial decomposition rate (W_0), maximum decomposition rate (W_M), and time to maximum decomposition rate (t_M) at different temperatures from the obtained standard volume of gas evolved (V_H) and decomposition rate (dV_H/dt) vs. time (t) curves shown in Figs. 2–5 and the values of apparent activation energy E_a obtained by differential and integral isoconversional non-linear equations (20) ~ (22) tabulated in Table 2. These E values are used to check the validity of the values of apparent activation energy E_a obtained by non-isothermic method. Because the E_a values calculated approach to those obtained by Kissinger's method and Ozawa's method, we conclude that the values of E_K , E_{op} and E_{oe} obtained are tenable.

$$\Omega_{isol}(E_a) = \min \left| \sum_i^n \sum_{i \neq j}^n \frac{t_i e^{-E_a/RT_{\alpha,i}}}{t_j e^{-E_a/RT_{\alpha,j}}} - n(n-1) \right| \quad (20)$$

$$\Omega_{isoD/k}(E_a) = \min \left| \sum_i^n \sum_{i \neq j}^n \frac{k_i e^{-E_a/RT_{\alpha,i}}}{k_j e^{-E_a/RT_{\alpha,j}}} - n(n-1) \right| \quad (21)$$

$$\Omega_{isoD/W}(E_a) = \min \left| \sum_i^n \sum_{i \neq j}^n \frac{W_i e^{E_a/RT_{\alpha,i}}}{W_j e^{E_a/RT_{\alpha,j}}} - n(n-1) \right| \quad (22)$$

**Fig. 2** The curves of change in gas formation with time during the thermal decomposition of BTNEDA with the loading density of $1 \times 10^{-3} \text{ g} \cdot \text{mL}^{-1}$ at various temperatures**Fig. 3** The curves of change in rate with time during the thermal decomposition of BTNEDA at 130 °C and 140 °C

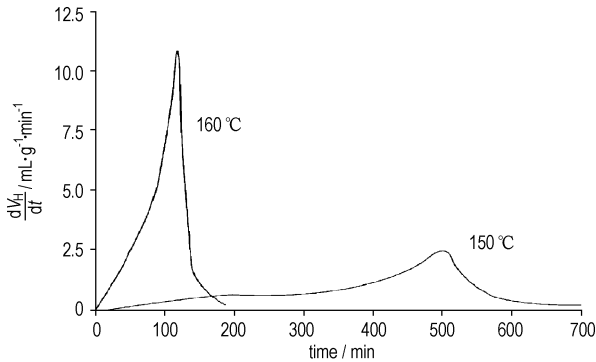


Fig. 4 The curves of change in rate with time during the thermal decomposition of BTNEDA at 150 °C and 160 °C

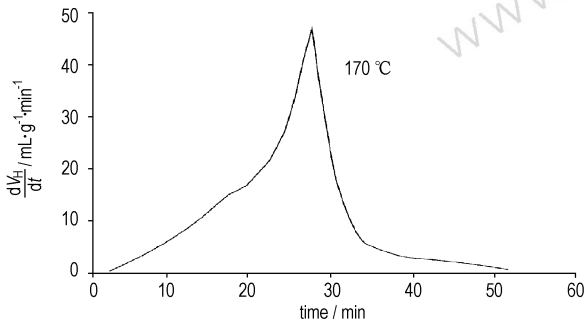


Fig. 5 The curve of change in rate with time during the thermal decomposition of BTNEDA at 170 °C

Table 2 The apparent activation energy obtained by characteristic data of the thermal decomposition reaction of BTNEDA at different temperatures¹⁾

characteristic data	temperature /°C							$E_a^{(2)}$
	130	135	140	145	150	160	170	/kJ·mol ⁻¹
$t_{1/2}$ /min	9540	1607		449.5	110.3	26.0	215.31	
W_0 /mL·(g·min) ⁻¹	0.001			0.032	0.090	0.30	211.82	
W_{M1} /mL·(g·min) ⁻¹	0.02107	0.1665		0.6924	2.198	11.78	226.51	
W_{M2} /mL·(g·min) ⁻¹	0.2402	0.6950		2.500	10.87	44.5	195.55	
t_M /min	10300	1910		497	120	26.9	217.81	

Note: 1) $t_{1/2}$, the half decomposition period; W_0 , the initial decomposition rate; W_M , the maximum decomposition rate; t_M , the time to maximum decomposition rate.

2) The data are obtained by differential and integral isoconversional non-linear methods^[21-22].

3.8 Self-accelerating decomposition temperature T_{SADT}

Setting T_0 as the initial decomposition temperature, at which the DSC curve deviates from the baseline, T_e as the onset temperature and T_p as the peak temperature, and defining $T_{e0 \text{ or } p0}$ as the value of $T_{(e0 \text{ or } p0)i}$ corresponding to $\beta \rightarrow 0$ and T_{e0} as the self-accelerating decomposition temperature T_{SADT} , we have

$$T_{0 \text{ or } e \text{ or } p} = T_{00 \text{ or } e0 \text{ or } p0} + b\beta_i + c\beta_i^2 + d\beta_i^3, \quad i=1, 2, \dots, L \quad (23)$$

$$\text{and } T_{e0} = T_{SADT} \quad (24)$$

The values of T_{00} , T_{e0} and T_{p0} obtained by using linear regression of T_{0i} , T_{ei} and T_{pi} against β_i as described in Eq. (23) are all listed in Table 1. The value of T_{SADT} of 440.73 K is obtained by the value of T_{e0} in Table 1 and Eq. (24).

3.9 Critical temperature of thermal explosion T_b

The critical temperature of thermal explosion (T_b) is an important parameter of evaluating the safety and elucidating transition tendency from thermal decomposition to thermal explosion for small-scale EMs.

For BTNEDA, the values of T_b obtained by Zhang-Hu-Xie-Li equation [Eq. (25)] taken from Ref. [23] using the values of T_{e0} and T_{p0} , and the value of E_{oe} and E_{op} listed in Table 1 are 449.88 and 455.28 K, respectively:

$$T_{be0 \text{ (or } bp0)} = \frac{E_{oe \text{ or } op} - \sqrt{E_{oe \text{ or } op}^2 - 4E_{oe \text{ or } op}RT_{e0 \text{ (or } p0)}}}{2R} \quad (25)$$

The values of T_b obtained by Hu-Yang-Liang-Xie equation [Eq. (26)] taken from Refs. [24-25] using the values of T_{00} , T_{e0} or T_{p0} , E_{op} (or E_{oe}) listed in Table 1 are 446.69 and 452.92 K, respectively.

$$\frac{E_{oe \text{ (or } op)}(T_{be0 \text{ (or } bp0)} - T_{00}) + 2RT_{be0 \text{ (or } bp0)}T_{00} - E_{oe \text{ (or } op)}(T_{be0 \text{ (or } bp0)} - T_{e0})}{RT_{be0 \text{ (or } bp0)}^2 + E_{oe \text{ (or } op)}(T_{be0 \text{ (or } bp0)} - T_{00})} = 1 \quad (26)$$

The values of T_b obtained by Eq. (27)^[18,26] based on Berthelot's equation using the values of b_{e0} and T_{e0} , b_{p0} and T_{p0} listed in Table 1 are 449.76 and 455.14 K, respectively.

$$T_{be0 \text{ (or } bp0)} = T_{e0 \text{ (or } p0)} + \frac{1}{b_{e0 \text{ (or } p0)}} \quad (27)$$

The values of T_b obtained by Eq. (28)^[10,27] based on Harcourt-Esson's equation using the values of a_{e0} and T_{e0} , a_{p0} and T_{p0} listed in Table 1 are 449.76 K and 455.14 K, respectively.

$$T_{be0 \text{ (or } bp0)} = \frac{a_{e0 \text{ (or } p0)}}{a_{e0 \text{ (or } p0)} - 1} T_{e0 \text{ (or } p0)} \quad (28)$$

The values of T_b obtained by Eq. (29)^[18,28] based on Berthelot's equation containing T_0 using the values of b and T_{e0} and T_{00} listed in Table 1 is 439.81 K.

$$b(T_b - T_{e0}) \left[1 + \frac{1}{1 + (T_b - T_{00})b} \right] = 1 \quad (29)$$

The values of T_b obtained by Eq. (30)^[18,29] based on Harcourt-Esson's equation containing T_0 using the values of a and T_{e0} and T_{00} listed in Table 1 is 435.75 K.

$$(T_b - T_{e0}) \left[\frac{\frac{a}{T_b} - \frac{a}{T_b^2}(T_b - T_{00})}{\frac{a}{T_b} + \frac{1}{1 + (T_b - T_{00})\frac{a}{T_b}}} \right] = 1 \quad (30)$$

It can be seen from the above-mentioned results that the calculated values of $T_{be0 \text{ (or } bp0)}$ obtained by the six different formulae agree well to each other, demonstrating that (1) for BTNEDA, the value of T_{be0} of 445.28 K and T_{bp0} of 454.62 K are acceptable; (2) Eqs. (25) - (30) are suitable for estimating the values of T_b for small-scale EMs; (3) In comparison with RDX with $T_b = 449.01$ K, the value of T_b of 454.62 K for BTNEDA shows that it has better thermal sensitivity.

3.10 Adiabatic time-to-explosion t_{Tlad}

The adiabatic time-to-explosion (t_{Tlad}) of EMs is the time of EM decomposition transiting to explosion under the adiabatic conditions and is an important parameter for assessing the thermal stability and the safety of EMs. In order to acquire the value of t_{Tlad} of BTNEDA, substituting the following data:

$$c_p = 1.12 \text{ J} \cdot \text{g}^{-1} \cdot \text{K}^{-1}, \quad Q_d = 3226 \text{ J} \cdot \text{g}^{-1}, \quad A_K = 10^{20.45} \text{ s}^{-1},$$

$$E = E_K = 199500 \text{ J} \cdot \text{mol}^{-1}, \quad R = 8.314 \text{ J} \cdot \text{mol}^{-1} \cdot \text{K}^{-1},$$

$f(\alpha) = 3(1 - \alpha)^{2/3}$, $T_0 = T_{e0} = 440.73$ K, $T = T_b = 455.26$ K into Eqs. (31) – (33)^[24,30].

$$c_p \frac{dT}{dt} = Q_d A \exp\left(-\frac{E}{RT}\right) f(\alpha) \quad (31)$$

$$t_{\text{Tlad}} = \int_0^t dt = \frac{1}{Q_d A} \int_{T_0}^T \frac{c_p \exp(E/RT)}{f(\alpha)} dT \quad (32)$$

$$\alpha = \frac{1}{Q_d A} \int_{T_0}^T \frac{c_p}{Q_d} dT \quad (33)$$

the value of t_{Tlad} of 1.25 s is obtained.

3.11 Critical temperature of hot-spot initiation $T_{\text{cr, hot-spot}}$

In order to obtain the critical temperature of hot-spot initiation ($T_{\text{cr, hot-spot}}$) of BTNEDA, assuming that $T_{\text{cr, hot-spot}}$ is a function of the size and duration of the hot-spot and of the physical and chemical properties of the explosive, the equation^[18,30–32] for calculating the value of $T_{\text{cr, hot-spot}}$ may be expressed as

$$\left(\frac{4}{3}\pi a^3\right) \rho Q_d \{1 - \exp[-(t - t_0) A e^{-E/RT_{\text{cr}}}] \} = \int_a^\infty 4\pi r^2 \rho c_p \left[\frac{a \theta_0}{r} \operatorname{erfc}\left[\frac{r-a}{\sqrt{2\lambda t}}\right] \right] dr \\ = \int_a^\infty 4\pi r^2 \rho c_p \left[\frac{a(T_{\text{cr, hot-spot}} - T_{\text{room}})}{r} \operatorname{erfc}\left[\frac{r-a}{\sqrt{\frac{\lambda}{\rho c_p} t}}\right] \right] dr \quad (34)$$

where a is the radius of the hot-spot in cm; ρ is the density in $\text{g} \cdot \text{cm}^{-3}$; Q_d is the heat of reaction in $\text{J} \cdot \text{g}^{-1}$; $t - t_0$ is the time interval in s; A is the frequency factor in s^{-1} ; E is the activation energy in $\text{J} \cdot \text{mol}^{-1}$; R is the gas constant in $\text{J} \cdot \text{mol}^{-1} \cdot \text{K}^{-1}$; $T_{\text{cr, hot-spot}}$ is the critical temperature of hot-spot initiation in K; c_p is the specific heat capacity in $\text{J} \cdot \text{g}^{-1} \cdot \text{K}^{-1}$; T_{room} is the ambient temperature in K; λ is the thermal conductivity in $\text{J} \cdot \text{cm}^{-1} \cdot \text{s}^{-1} \cdot \text{K}^{-1}$.

By substituting the following data of BTNEDA: $a = 10^{-3}$ cm, $\rho = 1.87$ $\text{g} \cdot \text{cm}^{-3}$, $Q_d = 3226$ $\text{J} \cdot \text{g}^{-1}$, $t - t_0 = 10^{-4}$ s, $A = A_K = 10^{20.45}$ s^{-1} , $E = E_K = 199.5$ $\text{kJ} \cdot \text{mol}^{-1}$, $R = 8.314$ $\text{J} \cdot \text{mol}^{-1} \cdot \text{K}^{-1}$, $c_p = 1.12$ $\text{J} \cdot \text{g}^{-1} \cdot \text{K}^{-1}$, $T_{\text{room}} = 293.15$ K, $\lambda = 26.9 \times 10^{-4}$ $\text{J} \cdot \text{cm}^{-1} \cdot \text{s}^{-1} \cdot \text{K}^{-1}$ into Eq. (34), the value of $T_{\text{cr, hot-spot}}$ of 333.86 °C is obtained.

3.12 Characteristic drop height of impact sensitivity H_{50}

To obtain the characteristic drop height of impact sensitivity (H_{50}) of BTNEDA, by substituting the values of λ , ρ , A , Q_d and E of eight explosives with known 50% drop height listed in

Table 3 into Eq. (35)^[18,33–34], the corresponding values of n of 0.564623, and of D_2 of 33.8765, and of D_3 of -0.347174 are obtained. By substituting the values of λ , ρ , A , Q_d and E of BTNEDA listed in Table 7 and the values of n , D_2 and D_3 into Eq. (35), the value of H_{50} of 15.03 cm of BTNEDA is obtained, showing that it has impact sensitivity level approaching those of PETN and tetryl (data seen Table 7).

$$\frac{1}{2} n \lg H_{50} + \lg \sqrt{\frac{\lambda}{\rho Q_d}} + D_3 + \frac{0.02612E}{T_1 + D_2 H_{50}^n} \quad (35)$$

where n , D_2 and D_3 are parameters of the correlation.

3.13 Critical thermal explosion ambient temperature T_{acr} , thermal sensitivity probability density function $S(T)$, safety degree SD and thermal explosion probability P_{TE}

In order to explore the heat-resistance ability of BTNEDA, the values of T_{acr} , $S(T)$ vs T relation, SD and P_{TE} are calculated by Frank-Kamenetskii formula (36)^[35] and Wang-Du's formulas (37) ~ (42)^[36–37]. In formulas (36) ~ (42), T_{acr} is the critical thermal explosion ambient temperature in K; E is the activation energy in $\text{J} \cdot \text{mol}^{-1}$; A is the pre-exponential constant in s^{-1} ; R is the gas constant in 8.314 $\text{J} \cdot \text{mol}^{-1} \cdot \text{K}^{-1}$; λ is the thermal conductivity in $\text{W} \cdot \text{m}^{-1} \cdot \text{K}^{-1}$; δ_{cr} is the Frank-Kamenetskii (FK) parameter; δ_{cr} is the criticality of thermal explosion of exothermic system; r is characteristic measurement of reactant in m; Q_d is decomposition heat in $\text{J} \cdot \text{kg}^{-1}$; ρ is density in $\text{kg} \cdot \text{m}^{-3}$; μ_T is the average value of temperature, K; σ_δ is the standard deviation of FK parameter; σ_T is the standard deviation of ambient temperature; T is surrounding temperature; $S(T)$ is the thermal sensitivity probability density function; SD is safety degree; P_{TE} is thermal explosion probability.

Substituting E with 199500 $\text{J} \cdot \text{mol}^{-1}$, A with $10^{20.45}$ s^{-1} , ρ with 1.87×10^3 $\text{kg} \cdot \text{m}^{-3}$, λ with 0.269 $\text{W} \cdot \text{m}^{-1} \cdot \text{K}^{-1}$, Q_d with 3.226×10^6 $\text{J} \cdot \text{kg}^{-1}$, r with 1.0 m, T with 350 K, σ_T with 10 K in Eqs. (36) ~ (42), $S(T)$ vs. T relation curves for infinite plate, infinite cylindrical and spheroidal BTNEDA in Fig. 6 and the maximum value of $S(T)$ vs T relation curve ($T_{S(T)\text{max}}$), SD , T_{acr} and P_{TE} of BTNEDA in Table 4 are obtained, showing that the thermal safety and the accelerating tendency from adiabatic decomposition to explosion of BTNEDA.

Table 3 Explosive parameters and comparison of experimental and predicted 50% drop heights (H_{50})

No.	acronym	$\lambda^{1)} 10^4$ / $\text{J} \cdot \text{cm}^{-1} \cdot \text{s}^{-1} \cdot \text{K}^{-1}$	ρ / $\text{g} \cdot \text{cm}^{-3}$	$\log(A/\text{s}^{-1})^{2)}$	$Q_d^{3)}$ / $\text{J} \cdot \text{g}^{-1}$	$E^{2)}$ / $\text{J} \cdot \text{mol}^{-1}$	H_{50}/cm		n	D_2	D_3
							Exp. ¹⁾	predicted			
1	HMX	34.43	1.79	33.80	2764	373700	32	33.4	0.564623	33.8765	-0.347174
2	RDX	10.58	1.66	12.50	2810	140000	26	20.1			
3	TNT	21.30	1.57	11.10	1506	155017	59	56.4			
4	PETN	25.10	1.68	10.40	3263	112300	16	15.60			
5	BTF	20.92	1.81	22.81	2949	255000	28	30.0			
6	HNS	8.53	1.65	22.63	1389	289000	54	50.1			
7	Tetryl	18.74	1.67	16.90	1904	172500	17 ⁴⁾	17.6			
8	NG	12.55	1.60	16.09	2092	150122	7 ⁴⁾	9.4			
9	BTNEDA	26.90	1.87	20.45	3226	199500	–	15.03			

Note: 1) cited from Ref. [1]; 2) cited from Ref. [2]; 3) Q_d taking a half of the explosion heat; 4) cited from Ref. [33]

Table 4 The calculated values of $T_{S(T)\text{max}}$, SD , T_{acr} and P_{TE} for BTNEDA

infinite cylinder			sphere				infinite plate				
$T_{S(T)\text{max}}/\text{K}$	T_{acr}/K	$P_{\text{TE}}/\%$	$SD/\%$	$T_{S(T)\text{max}}/\text{K}$	T_{acr}/K	$P_{\text{TE}}/\%$	$SD/\%$	$T_{S(T)\text{max}}/\text{K}$	T_{acr}/K	$P_{\text{TE}}/\%$	$SD/\%$
354.5	349.73	60.69	39.31	357.0	352.42	54.19	45.81	350.0	345.47	71.45	28.55

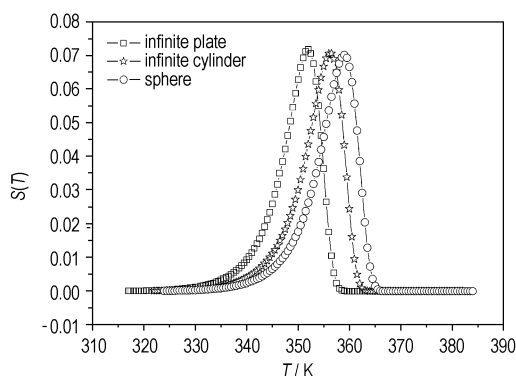


Fig. 6 The $S(T)$ vs. T relation curves for infinite platelike, infinite cylindrical and spheroidal BTNEDA

$$T_{acr} = \frac{-E_k}{2RLambertW_{-1}\left(-\frac{1}{2}\sqrt{\frac{\lambda E_k \delta_{cr}}{r^2 Q_d \rho A_k R}}\right)} \quad (36)$$

$$S(T) = \frac{W(E_k - 2RT)}{\sqrt{2\pi\sigma_\delta RT^4}} \exp\left\{-\left[W\frac{\exp\left(-\frac{E_k}{RT}\right)}{T^2} - \delta_{cr}\right]^2 / 2\sigma_\delta^2 - \frac{E_k}{RT}\right\} \quad (37)$$

$$\text{where } \frac{r^2 Q_d E_k \rho A_k}{\lambda R} = W \quad (38)$$

$$\sigma_\delta = W\left(\frac{E_k - 2R\mu_T}{R\mu_T^4}\right) \exp\left(-\frac{E_k}{R\mu_T}\right) \sigma_T \quad (39)$$

$$\mu_T = \frac{-E_k}{2RLambertW_{-1}\left(-\frac{1}{2}\sqrt{\frac{\lambda E_k \delta_{cr}}{r^2 Q_d \rho A_k R}}\right)} \quad (40)$$

And σ_δ is the standard derivation of Frank-Kamenetskii parameter, σ_T is the standard derivation of the measured surrounding temperature and μ_T is the mean value of T .

SD was obtained by Eq. (41)

$$SD = \int_0^{+\infty} \int_0^{+\infty} \frac{W(E_k - 2RT)}{\sqrt{2\pi\sigma_\delta RT^4}} \exp\left\{-\left[W\frac{\exp\left(-\frac{E_k}{RT}\right)}{T^2} - \delta_{cr}\right]^2 / 2\sigma_\delta^2 - \frac{E_k}{RT} - \frac{(Y - T + \mu_T)^2}{2\sigma_T^2}\right\} dT dY \quad (41)$$

The thermal explosion probability (P_{TE}) was expressed as Eq. (42)

$$P_{TE} = 1 - SD \quad (42)$$

3.14 IR frequencies and NMR chemical shifts

Vibrational frequencies were calculated after stationary points were located in order to ascertain that the structure obtained corresponds to a minimum on the potential energy surface. In the result of frequency calculation, there is no imaginary frequency which indicates that our optimized geometry is the stable one. To verify the suitability of the basis set we used, single-point calculations were further carried out with the aug-cc-pvdz basis set. The total energy calculated with 6-311 + +G** basis set is -1984.2167852 hartree and that with aug-cc-pvdz basis set is -1983.9525405 hartree which indicates that the results are not greatly affected by basis set size.

From the optimized geometry (Fig. 7), one can conclude that the whole molecule has an inversion center in the center C—C bond and the atoms are symmetric about the center.

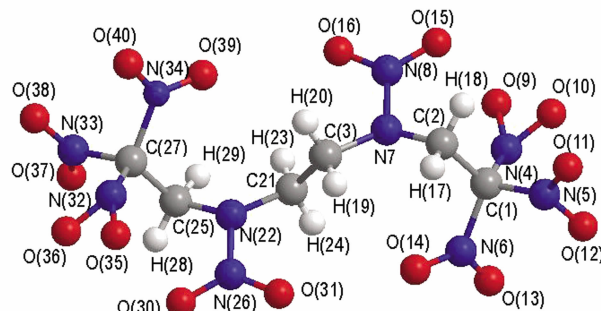


Fig. 7 optimized structure of BTNEDA

Based on the simple harmonic oscillator analysis, 3N—6 (the number of atom is 40) frequencies and intensities of 114 frequencies were obtained, only those larger than 600 cm^{-1} were listed in Table 5. The scaled IR frequencies were calibrated by multiplying 0.96. For the complexity of vibrational mode, it is difficult to assign all bands, so we have only analyzed some typical vibrational modes comparing with those of the experimental. The theoretical value at 1299 cm^{-1} is caused by C—H stretching vibration. The asymmetric characteristic absorption peaks of C—NO₂ are found to be at 1285 and 1292 cm^{-1} . The asymmetric characteristic absorption peaks of C—H are found to be at 3017 and 3023 cm^{-1} . The stretching vibration of N—NO₂ is found to be at 1245 cm^{-1} .

Table 5 The scaled IR frequencies for BTNEDA

ν /cm ⁻¹	I /km · mol ⁻¹	ν /cm ⁻¹	I /km · mol ⁻¹	ν /cm ⁻¹	I /km · mol ⁻¹
602	6	963	40	1370	15
616	11	983	4	1372	8
651	2	988	7	1391	12
653	2	1036	17	1401	33
662	16	1052	85	1424	22
695	9	1071	1	1433	41
709	5	1127	37	1565	400
725	4	1175	13	1577	125
725	29	1220	23	1587	138
738	24	1245	210	1590	451
752	7	1260	340	1605	730
760	11	1285	176	1609	112
790	23	1286	214	1620	260
792	71	1286	0	1622	232
818	131	1290	43	2945	9
822	30	1292	152	2964	9
835	47	1299	41	2965	3
836	6	1308	33	2986	2
839	34	1320	17	3006	0
854	64	1326	20	3017	10
911	109	1334	1	3023	20
928	13	1340	4	3038	2
940	12	1364	32		

3.15 Population analysis

From Table 6, we can see that the molecule has an inversion center in the center C(21)—C(3) bond and all the C—C bonds are of antibonding molecule orbital, the overlap

between C—C bonds are very largest. The overlap between N(7)—C(3) and N(22)—C(21) are lowest and these two bonds will be broken firstly.

Table 6 Population analysis of BTNEDA

bonds	population	bonds	population
C(1)—C(2)	-24.2797	C(25)—C(27)	-24.2797
C(1)—N(4)	-5.2672	C(27)—N(32)	-5.2672
C(1)—N(5)	-1.0017	C(27)—N(33)	-1.0017
C(1)—N(6)	-6.3534	C(27)—N(34)	-6.3534
C(2)—N(7)	0.7919	C(25)—N(22)	0.7919
N(7)—N(8)	-3.5066	N(22)—N(26)	-3.5066
N(7)—C(3)	-0.7030	N(22)—C(21)	-0.7030
C(3)—C(21)	-8.7750		

3.16 Atomic Charges

From Table 7, we can see that the charges of all the carbon atoms are negative. All the charges on N(N(7) and N(22)) which are connected with a nitro-group are positive and carry large charges (0.927080e), those on two N atoms of NO₂ are positive while those on the other four N atoms of NO₂ are negative. From the total atomic charge calculation of —NO₂, the total atomic charges of —NO₂ on C—NO₂ carry positive charges of 0.040974e (N(33), O(37), O(38)), 0.25827e (N(34), O(39), O(40)), 0.05788e (N(32), O(35), O(36)) while the total atomic charges of —NO₂ on N—NO₂ carry negative charges of -0.55683e (N(26), O(30), O(31)), since the NO₂ connected with different atoms.

Table 7 Mulliken net charges of BTNEDA

atoms	charges/e	atoms	charges/e
C(1)	-0.520740	C(27)	-0.520740
C(2)	-0.488207	C(25)	-0.488207
C(3)	-0.796312	C(21)	-0.796312
N(4)	-0.092293	N(32)	-0.092293
N(5)	-0.130489	N(33)	-0.130489
N(6)	0.164160	N(34)	0.164160
N(7)	0.927080	N(22)	0.927080
N(8)	-0.644464	N(26)	-0.644464
O(9)	0.026025	O(35)	0.026025
O(10)	0.124148	O(36)	0.124148
O(11)	0.068473	O(37)	0.068473
O(12)	0.102990	O(38)	0.102990
O(13)	0.034594	O(39)	0.034594
O(14)	0.059516	O(40)	0.059516
O(15)	0.029329	O(30)	0.029329
O(16)	0.058302	O(31)	0.058302
H(17)	0.290125	H(28)	0.290125
H(18)	0.328260	H(29)	0.328260
H(19)	0.232199	H(23)	0.232199
H(20)	0.227303	H(24)	0.227303

3.17 Frontier Orbital Energy Analysis

Based on the composition of the molecule and the basis set we selected, there are 121 occupied molecule orbitals and 639 unoccupied molecule orbitals. According to the MO theory, the Highest Occupied Molecular Orbital (HOMO) and

the Lowest Unoccupied Molecular Orbital (LUMO) are the most important factors that affect the properties of compounds. Studying the frontier orbital energy can provide good information about the properties of compounds. The frontier energy gap ($\Delta E = E_{\text{LUMO}} - E_{\text{HOMO}} = -0.15610 - (-0.32544)$) for BTNEDA is 0.16934 Hartree which indicates that the compound is stable in some extent. The frontier orbitals of BTNEDA were shown at Fig. 8. The main compositions of HOMO in the compound are the atoms of C(2), C(3), C(21) and C(25), the nitro-groups of N(7) and N(22), while the main compositions of LUMO are four nitro-groups of N(4), N(5), N(32) and N(33) atoms.

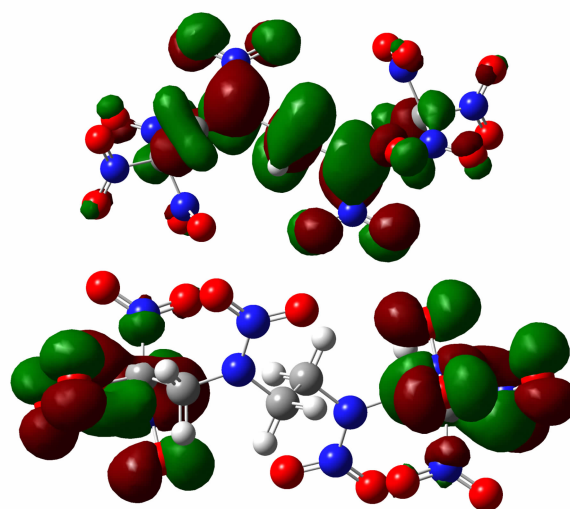


Fig. 8 HOMO and LUMO of BTNEDA

4 Conclusions

(1) $\Delta_c U_{(\text{BTNEDA}, s, 298.15\text{K})} = -(3478.11 \pm 6.41) \text{ kJ} \cdot \text{mol}^{-1}$ and $\Delta_f H_m^{\theta}(\text{BTNEDA}, s, 298.15\text{K}) = -(53.54 \pm 6.41) \text{ kJ} \cdot \text{mol}^{-1}$.

(2) $T_{\text{bp0}}(\text{BTNEDA}) = 454.62 \text{ K}$, $T_{\text{bp0}}(\text{RDX}) = 449.01 \text{ K}$, showing that BTNEDA has better thermal sensitivity.

(3) $D_{(\text{BTNEDA})} = 9.298 \text{ km} \cdot \text{s}^{-1}$ ($\rho = 1.87 \text{ g} \cdot \text{cm}^{-3}$), $\rho_{(\text{BTNEDA})} = 39.23 \text{ GPa}$, $D_{(\text{HMX})} = 9.041 \text{ km} \cdot \text{s}^{-1}$ ($\rho = 1.877 \text{ g} \cdot \text{cm}^{-3}$), $\rho_{(\text{HMX})} = 37.17 \text{ GPa}$, $H_{50}(\text{BTNEDA}) = 15.03 \text{ cm}$, $H_{50}(\text{PETN}) = 15.60 \text{ cm}$, $H_{50}(\text{Tetryl}) = 17.60 \text{ cm}$, $T_{\text{cr, hot-spot}}(\text{BTNEDA}) = 333.86 \text{ }^{\circ}\text{C}$, indicating that BTNEDA has explosion performance level approaching that of HMX. It is sensitive to shock, and has impact sensitivity level approaching those of PETN and tetryl.

(4) The theoretical calculation indicated that the whole molecule has an inversion center in the center C—C bond and the atoms are symmetric about the center, and the overlap between N(7)—C(3) and N(22)—C(21) are lowest and these two bonds will be broken firstly.

References:

- [1] DONG Hai-shan, ZHOU Fen-fen. Properties of high explosives and related materials [M]. Beijing: Science Press, 1989, (in Chinese).
- [2] DONG Hai-shan, HU Rong-zu, YAO Pu, et al. Collection of thermospectrum of energetic materials [M]. Beijing: National Defense Industry Press, 2002. (in Chinese).

- [3] CHEN San-ping, HU Rong-zu, SONG Ji-rong, et al. Thermal behavior of *N,N'*-bis[*N*-(2,2,2-trinitroethyl)-*N*-nitro]ethylenediamine[J]. *Chin J Chem*, 2004, 22(7): 658–660.
- [4] SONG Quan-cai, HU Rong-zu, ZHAO Feng-qi, et al. Differential and integral isoconversional non-linear methods and their application in physical chemistry study of energetic materials—II. Thermal decomposition of TNMA, BTNEDA AND TNETB [J]. *Chin J Energ Mater*, 2007, 15(3): 193–195 (in Chinese).
- [5] HU Rong-zu, SONG Quan-cai, DONG Hai-shan, et al. Kinetic parameters of explosive decomposition reaction of trinitromethyl explosives as a function of temperature[J]. *Chin J Explos Propel*, 2009, 32(6): 62–65.
- [6] HU Rong-zu, GAO Hong-xu, ZHAO Feng-qi, et al. The estimation of critical temperatures of hot-spot initiation in energetic materials[J]. *Chin J Energ Mater (Hanneng Cailiao)*, 2009, 17(2): 127–130 (in Chinese).
- [7] HU Rong-zu. Note on Bourdon manometer and its experimental data processing[J]. *Explosive Materials*, 1966(4): 54–60.
- [8] HU Rong-zu, LU Xing-sen, FANG Yin-gao. Thermal behaviour of 2,4,6,8,10,12-hexanitro-2,4,6,8,10,12-hexaazatricyclo[7.3.0.0^{3,7}]dodecane-5,11-dione [J]. *J Energ Mater*, 1993, 11(3): 219–244.
- [9] HU Rong-zu, XIE Jun-jie. Investigation of the ingredients compatibility and available life of the plastic bonded explosives (PBX) [C] // Jt. Symp. Compat. Plast. /Mater. Explos. Process. Explos. 1980: 335–48.
- [10] XIAO He-ming, JU Xue-hai, XU Li-na, et al. A density – functional theory investigation of 3-nitro-1,2,4-triazole-5-one dimers and crystal[J]. *Journal of Chemical Physics*, 2004, 121(24): 12523–12531.
- [11] MA Hai-xia, SONG Ji-rong, XIAO He-ming, et al. Density functional theoretical investigation on 3,4-dinitrofurazanfuroxan [J]. *Chinese Journal of Explosives and Propellants*, 2006, 29: 43–46, 61.
- [12] MA Hai-xia, SONG Ji-rong, HU Rong-zu, et al. Molecular structure, the quantum chemical investigation and the thermal behavior of dimethylamine salt of 3-nitro-1,2,4-triazol-5-one ($(\text{CH}_3)_2\text{NH}_2^+ \text{C}_2\text{N}_4\text{O}_3\text{H}^-$) [J]. *J Molecule Structure (THEOCHEM)*, 2004, 678: 217–222.
- [13] Curtiss L A, McGrath M P, Blaudeau J P, et al. Extension of Gaussian-2 theory to molecules containing third-row atoms Ga-Kr [J]. *J Chem Phys*, 1995, 103: 6104–6113.
- [14] Clark T, Chandrasekhar J, Spitznagel G W, et al. Efficient diffuse function-augmented basis sets for anion calculations. III. The 3-21+G basis set for first-row elements [J]. *J Comp Chem*, 1983, 4: 294–301.
- [15] Frisch M J, Pople J A, Binkley J S. Self-consistent molecular orbital methods 25. Supplementary functions for Gaussian basis sets [J]. *J Chem Phys*, 1984, 80: 3265–3269.
- [16] Wong M W. Vibrational Frequency Prediction Using Density Functional Theory [J]. *Chem Phys Letters*, 1996, 256: 391–399.
- [17] Frisch M J, Trucks G W, Schlegel H B, et al. Gaussian 03 (Revision B.01) [G]. Gaussian, Inc., Pittsburgh PA, 2003.
- [18] HU Rong-zu, ZHAO Feng-qi, GAO Hong-xu, et al. Fundamentals and application of calorimetry [M]. Beijing: Science Press, 2010.
- [19] Kissinger H E. Reaction kinetics on differential thermal analysis [J]. *Anal Chem*, 1957, 29(11): 1702–1706.
- [20] Ozawa T. A new method of analyzing thermogravimetric data [J]. *Bull Chem Soc Jpn*, 1965, 38(1): 1881–1886.
- [21] HU Rong-zu, ZHAO Feng-qi, GAO Hong-xu, et al. Differential and integral isoconversional non-linear methods and their application in physical chemistry study of energetic materials. Theory and method [J]. *Chinese Journal of Energetic Materials*, 2007, 15(2): 97–100.
- [22] HU Rong-zu, SHI Qi-zheng. Thermal Analysis Kinetics [M]. Beijing: Science Press, 2001.
- [23] ZHANG Tong-lai, HU Rong-zu, XIE Yi, et al. The estimation of critical temperature of thermal explosion for energetic materials using non-isothermal DSC [J]. *Thermochim Acta*, 1994, 244(2): 171–176.
- [24] HU Rong-zu, GAO Sheng-li, ZHAO Feng-qi, et al. Thermal analysis kinetics [M]. Beijing: Science Press, 2008.
- [25] XIE Yi, HU Rong-zu, YANG Chao-qing, et al. Studies on the critical temperature of thermal explosion for 3-nitro-1,2,4-triazol-5-one (NTO) and its salts [J]. *Propellants, Explosives, Pyrotechnics*, 1992, 17(6): 298–302.
- [26] XUE Liang, ZHAO Feng-qi, HU Rong-zu, et al. A simple method to estimate the critical temperature of thermal explosion for energetic materials using non-isothermal DSC [J]. *Journal Energetic Materials*, 2010, 28: 17–34.
- [27] ZHAO Feng-qi, HU Rong-zu, GAO Hong-xu. A simple method based on Harcourt-Esson's equation to estimate the critical temperature of thermal explosion for energetic materials using non-isothermal DSC [J]. *Chin J Chem*, 2009, 27: 1067–1072.
- [28] ZHAO Feng-qi, HU Rong-zu, ZHANG Hai, et al. Estimation of critical temperature of thermal explosion for energetic materials based on non-isothermal kinetic equation $d\alpha/dt = A_0 \exp(bT) [1 + (T - T_0)b] f(\alpha)$ [J]. *Chemical Research in Chinese Universities*, 2010, 26(5): 829–832.
- [29] ZHANG Hai, HU Jun-ying, HU Rong-zu, et al. A new method based on the non-isothermal kinetic equation to estimate the critical temperature of thermal explosion for energetic materials using non-isothermal DSC [J]. *Journal of Jiaotong University*, 2011, 16(2): 247–251.
- [30] Smith L C. An approximate solution of the adiabatic explosion problem [J]. *Thermochim Acta*, 1975, 13(1): 1–6.
- [31] Friedman M H. Size of "Hot spots" in the impact explosion of exothermic materials [J]. *Trans Faraday Soc*, 1963, 59: 1865–1873.
- [32] Bruckman H J, Guillet J E. Theoretical calculations of hot-spot initiation in explosives [J]. *Can J Chem*, 1968, 41: 3221–3228.
- [33] Friedman, M. A correlation of impact sensitivities by means of the hot model [C] // 9th (International) Symposium on Combustion, New York, Academic Press Inc., 1963: 294–302.
- [34] HU Rong-zu, ZHAO Feng-qi, GAO Hong-xu, et al. The estimation of characteristic drop heights of impact sensitivity for polymer bonded explosives JH-94 and JO-96 [J]. *Chin J Energ Mater*, 2009, 17(3): 251 (in Chinese).
- [35] Frank-Kamenetskii D A. Temperature distribution in reaction vessel and stationary theory of thermal explosion [J]. *J Phys Chem (USSR)*, 1939, 13(6): 738–755.
- [36] WANG Peng. Study on thermal safety and ignition reliability of exothermic system [D]. Beijing: Beijing Institute of Technology, 2008.
- [37] WANG Peng, DU Zhi-ming. Probability distribution of thermal sensitivity of energetic materials [J]. *Chin J Energ Mater (Hanneng Cailiao)*, 2007, 15(6): 633–636 (in Chinese).

N,N'-二[(2,2,2-三硝基乙基-*N*-硝基)]乙二胺的热安全性和密度泛函理论研究

胡荣祖^{1,3}, 赵凤起¹, 高红旭¹, 马海霞², 张海³, 徐抗震², 赵宏安⁴, 姚二岗¹

(1. 西安近代化学研究所燃烧与爆炸技术重点实验室, 陕西 西安 710065; 2. 西北大学化工学院, 陕西 西安 710069;

3. 西北大学数学系/数据分析和计算化学研究所, 陕西 西安 710069; 4. 西北大学信息科学与工程学院, 陕西 西安 710069)

摘要: 借助 *N,N'*-二[(2,2,2-三硝基乙基-*N*-硝基)]乙二胺的恒容标准燃烧热 (Q_c), 不同加热速率 (β) 非等温 DSC 曲线离开基线的初始温度 (T_0)、 onset 温度 (T_e)、最大峰顶温度, 由 Kissinger 法和 Ozawa 法所得的热分解反应活化能 (E_k , E_o) 和指前因子 (A_k), 从方程 $\ln\beta_i = \ln[A_0/b_{e0(or p0)} G(\alpha)] + b_{e0(or p0)} T_{e(or p)i}$ 所得的值 $b_{e0(or p0)}$, 从方程 $\ln\beta_i = \ln[A_0/(a_{e0(or p0)} + 1) G(\alpha)] + (a_{e0(or p0)} + 1) \ln T_{e(or p)i}$ 所得的 $a_{e0(or p0)}$ 值, 从方程 $\ln\left(\frac{\beta_i}{T_{ei} - T_{0i}}\right) = \ln\left(\frac{A_0}{G(\alpha)}\right) + bT_{ei}$ 所得的 b 值, 从方程 $\ln\left(\frac{\beta_i}{T_{ei} - T_{0i}}\right) = \ln\left(\frac{A_0}{G(\alpha)}\right) + a \ln T_{ei}$ 所得的 a 值, 估算的比热容 (c_p)、密度 (ρ)、热导率 (λ) 和分解热 (Q_d , 取爆热之半) 数据, Zhang-Hu-Xie-Li 公式, Hu-Yang-Liang-Xie 公式, 基于 Berthelot 方程和 Harcourt-Esson 方程计算热爆炸临界温度的公式, Smith 方程, Friedman 公式, Bruckman-Guillet 公式, 热力学公式和 Wang-Du 公式, 计算了由理想燃烧反应和 Hess 定律得到的 BTNEDA 的恒容标准燃烧能 $\Delta_c U_{(BTNEDA, s, 298.15K)}$ 和标准生成焓 $\Delta_f H_m^0 (BTNEDA, s, 298.15K)$, $\beta \rightarrow 0$ 时的 T_0 、 T_e 和 T_p 值 (T_{00} , T_{e0} 和 T_{p0}), 热爆炸临界温度 (T_{be0} 和 T_{bp0}), 绝热至爆时间 (t_{Tlad}), 撞击感度 50% 落高 (H_{50}), 热点起爆临界温度 (T_{cr}), 被 350 K 环境包围的半厚和半径为 1 m 的无限大平板、无限长圆柱和球形 BTNEDA 的热感度概率密度函数, 相应于 $S(T)$ 与 T 关系曲线最大值的峰温 ($T_{S(T)max}$), 安全度 (SD), 临界热爆炸环境温度 (T_{acr}) 和热爆炸概率 (P_{TE})。得到了评价 BTNEDA 热安全性的下列结果: (1) $\Delta_c U_{(BTNEDA, s, 298.15K)} = -(3478.11 \pm 6.41) \text{ kJ} \cdot \text{mol}^{-1}$ 和 $\Delta_f H_m^0 (BTNEDA, s, 298.15K) = -(53.54 \pm 6.41) \text{ kJ} \cdot \text{mol}^{-1}$; (2) $T_{00} = 438.73 \text{ K}$, $T_{SADT} = T_{e0} = 440.73 \text{ K}$, $T_{p0} = 446.53 \text{ K}$; $T_{be0} = 449.88 \text{ K}$, $T_{bp0} = 455.28 \text{ K}$; (3) 当 $E_k = 199.5 \text{ kJ} \cdot \text{mol}^{-1}$, $A_k = 10^{20.45} \text{ s}^{-1}$, $c_p = 1.12 \text{ J} \cdot \text{g}^{-1} \cdot \text{K}^{-1}$, $Q_d = 3226 \text{ J} \cdot \text{g}^{-1}$, $T_0 = T_{e0} = 440.73 \text{ K}$, $T = T_p = 455.26 \text{ K}$, $f(\alpha) = 3(1 - \alpha)^{2/3}$, $a = 10^{-3} \text{ cm}$, $\rho = 1.87 \text{ g} \cdot \text{cm}^{-3}$, $t - t_0 = 10^{-4} \text{ s}$, $T_{room} = 293.15 \text{ K}$ 和 $\lambda = 0.00269 \text{ J} \cdot \text{cm}^{-1} \cdot \text{s}^{-1} \cdot \text{K}^{-1}$, $H_{50} = 15.03 \text{ cm}$, $t_{Tlad} = 1.25 \text{ s}$, $T_{cr, hot, spot} = 333.86 \text{ K}$; 对无限大平板, $T_{S(T)max} = 350 \text{ K}$, $T_{acr} = 345.47 \text{ K}$, $SD = 28.55\%$, $P_{TE} = 71.45\%$; 对无限长圆柱, $T_{S(T)max} = 354.5 \text{ K}$, $T_{acr} = 349.73 \text{ K}$, $SD = 39.31\%$, $P_{TE} = 60.69\%$; 对球, $T_{S(T)max} = 357.00 \text{ K}$, $T_{acr} = 352.42 \text{ K}$, $SD = 45.81\%$, $P_{TE} = 54.19\%$ 。运用密度泛函理论计算获得了 BTNEDA 的优化构型及红外光谱, 分析了其分子总能量、前沿轨道能量和原子净电荷分布。

关键词: 物理化学; *N,N'*-二[(2,2,2-三硝基乙基-*N*-硝基)]乙二胺 (BTNEDA); 热分解; 热安全性; 自加速分解温度; 热爆炸临界温度; 绝热至爆时间; 撞击感度; 热点起爆临界温度; 安全度; 临界热爆炸环境温度; 热爆炸概率; 量子化学计算

中图分类号: TJ55; O643

文献标识码: A

DOI: 10.3969/j.issn.1006-9941.2012.05.001



追忆董海山院士

1962年,以周恩来总理为主任的中央专门委员会批准了二机部关于组织高能炸药协作攻关的请示报告。当年4月二机部九院(现中国工程物理研究院)、中科院兰州化学物理研究所、三机部第三研究所(现西安近代化学研究所)的有关科研人员,集中西安,大力协同,在西安近代化学研究所的标志性建筑——苏式大U楼内开始了高能炸药的研制工作。4年间,董海山博士作为这一研制工作的负责人、学术带头人和领军人物,以他的聪明才智,刻苦、奉献、敬业精神,严谨的学风,高尚的协作风格,留苏掌握的先进技术、经验,成功地仿制了1~9号硝仿系高能单质炸药,阐明了以硝仿为酸组分的曼尼希反应机理,发现了伯胺的三硝基乙基-*N*-亚硝基化反应,改进了10号炸药的合成工艺,填补了我国研制新型高能单质炸药的空白,促进了以后几十年含能材料合成的发展、高能炸药合成研究室、小型生产试制线的建立,带动了火炸药配方活性添加剂、理化分析、性能测试手段的配套研究,为我国含能材料科学技术和国防建设作出了重要贡献。

2012年,迎来了142任务50周年纪念和董海山院士诞辰80周年,为追忆青年董海山博士在西安三所4年工作的激情岁月,我们特选那时由他亲自合成的BTNEDA为研究对象,撰写了“BTNEDA的热安全和密度泛函理论研究”一文作纪念。

(西安近代化学研究所 朱春华 胡荣祖)